

3-2010

The *Pseudomonas syringae* type III effector HopG1 targets mitochondria, alters plant development, and suppresses plant innate immunity

Anna Block

University of Nebraska-Lincoln, ablock2@unl.edu

Ming Guo

University of Nebraska-Lincoln, mguo2@unl.edu

Guangyong Li

University of Nebraska-Lincoln, gli3@unl.edu

Christian Elowsky

University of Nebraska-Lincoln, celowsky@unl.edu

Thomas Clemente

University of Nebraska - Lincoln, tclemente1@unl.edu

See next page for additional authors

Follow this and additional works at: <https://digitalcommons.unl.edu/plantscifacpub>

 Part of the [Plant Biology Commons](#), [Plant Breeding and Genetics Commons](#), and the [Plant Pathology Commons](#)

Block, Anna; Guo, Ming; Li, Guangyong; Elowsky, Christian; Clemente, Thomas; and Alfano, James R., "The *Pseudomonas syringae* type III effector HopG1 targets mitochondria, alters plant development, and suppresses plant innate immunity" (2010). *Faculty Publications from the Center for Plant Science Innovation*. 136.
<https://digitalcommons.unl.edu/plantscifacpub/136>

This Article is brought to you for free and open access by the Plant Science Innovation, Center for at DigitalCommons@University of Nebraska - Lincoln. It has been accepted for inclusion in Faculty Publications from the Center for Plant Science Innovation by an authorized administrator of DigitalCommons@University of Nebraska - Lincoln.

Authors

Anna Block, Ming Guo, Guangyong Li, Christian Elowsky, Thomas Clemente, and James R. Alfano

Published in final edited form as:

Cell Microbiol. 2010 March ; 12(3): 318–330. doi:10.1111/j.1462-5822.2009.01396.x.

© 2009 Blackwell Publishing Ltd

The *Pseudomonas syringae* type III effector HopG1 targets mitochondria, alters plant development, and suppresses plant innate immunity

Anna Block^{1,2}, Ming Guo^{1,2}, Guangyong Li^{1,2}, Christian Elowsky³, Thomas E. Clemente^{1,3}, and James R. Alfano^{1,2}

¹The Center for Plant Science Innovation, University of Nebraska, Lincoln, Nebraska, United States of America

²Department of Plant Pathology, University of Nebraska, Lincoln, Nebraska, United States of America

³Center for Biotechnology, University of Nebraska, Lincoln, Nebraska, United States of America

Summary

The bacterial plant pathogen *Pseudomonas syringae* uses a type III protein secretion system to inject type III effectors into plant cells. Primary targets of these effectors appear to be effector-triggered immunity (ETI) and pathogen-associated molecular pattern (PAMP)-triggered immunity (PTI). The type III effector HopG1 is a suppressor of ETI that is broadly conserved in bacterial plant pathogens. Here we show that HopG1 from *P. syringae* pv. *tomato* DC3000 also suppresses PTI. Interestingly, HopG1 localizes to plant mitochondria, suggesting that its suppression of innate immunity may be linked to a perturbation of mitochondrial function. While HopG1 possesses no obvious mitochondrial signal peptide, its N-terminal two-thirds was sufficient for mitochondrial localization. A HopG1-GFP fusion lacking HopG1's N-terminal 13 amino acids was not localized to the mitochondria reflecting the importance of the N-terminus for targeting. Constitutive expression of HopG1 in *Arabidopsis thaliana*, *Nicotiana tabacum* (tobacco) and *Lycopersicon esculentum* (tomato) dramatically alters plant development resulting in dwarfism, increased branching and infertility. Constitutive expression of HopG1 *in planta* leads to reduced respiration rates and an increased basal level of reactive oxygen species. These findings suggest that HopG1's target is mitochondrial and that effector/target interaction promotes disease by disrupting mitochondrial functions.

Introduction

Many gram-negative phytopathogenic bacteria use a syringe-like apparatus called a type III secretion system (T3SS) to inject type III effector (T3E) proteins into plant cells to promote pathogenicity (Alfano & Collmer, 2004). The T3SS of the hemibiotrophic pathogen *Pseudomonas syringae* is encoded by the *hrp* and *hrc* genes located within the Hrp pathogenicity island and is often referred to as the Hrp T3SS (Alfano *et al.*, 2000). *P. syringae* pv. *tomato* DC3000 has become an important model pathogen as it infects both *Lycopersicon esculentum* (tomato) and the model plant *Arabidopsis thaliana* in a T3SS-dependent manner. Bioinformatic analysis of the DC3000 genome has led to the identification of over 30 T3Es most of whose activities and plant targets remain unknown (Lindeberg *et al.*, 2006). DC3000 mutants defective in their T3SS are nonpathogenic

reflecting the requirement of the T3Es for pathogenicity. However, pathogenesis of DC3000 mutants defective in individual T3Es is in general only slightly compromised, suggesting that many T3Es are functionally redundant. More recently it was discovered that a primary target for many *P. syringae* T3Es is the plant innate immune system (Abramovitch *et al.*, 2006, Espinosa & Alfano, 2004)

The plant innate immune system is composed of at least two branches (Jones & Dangl, 2006). First, extracellular plant receptors recognize conserved molecules on microorganisms called pathogen-associated molecular patterns (PAMPs) sometimes referred to as microbe-associated molecular patterns (MAMPs), which are present on pathogenic and non-pathogenic microbes (Nurnberger *et al.*, 2004, Ausubel, 2005). PAMP recognition activates plant innate immune responses that are collectively referred to as PAMP-triggered immunity (PTI). Several plant pathogen T3Es have been shown to suppress outputs of PTI (Alfano & Collmer, 2004, Chisholm *et al.*, 2006). Plants likely evolved the second branch of the plant innate immune system, referred to as effector-triggered immunity (ETI) (Jones & Dangl, 2006), to counter the ability of pathogen effectors to suppress PTI. ETI is based on the ability of resistance (R) proteins to recognize pathogen effectors resulting in the activation of innate immune pathways. There is overlap between the outputs of PTI and ETI (Tao *et al.*, 2003, Zipfel *et al.*, 2004, Tsuda *et al.*, 2008). However, ETI is generally considered a more substantial immune response that usually includes the hypersensitive response (HR), a form of programmed cell death (PCD) elicited upon microbial attack. Bacterial plant pathogen T3Es have also been shown to suppress ETI (Jamir *et al.*, 2004, Abramovitch *et al.*, 2003). The fact that some T3Es seem capable of suppressing both PTI and ETI suggests that these T3Es have multiple targets or that they are targeting shared components of PTI and ETI.

While the activities and targets for most plant pathogen T3Es remain unknown, there has been recent progress made for several *P. syringae* T3Es (Block *et al.*, 2008, Zhou & Chai, 2008, Cunnac *et al.*, 2009). Insight into the role that T3Es are playing in pathogenesis can be gained by elucidating their subcellular localization. For example, several *P. syringae* T3Es possess myristoylation sites, suggestive of membrane targeting. These include AvrRpm1 (Nimchuk *et al.*, 2000), AvrB (Nimchuk *et al.*, 2000), AvrPto (Shan *et al.*, 2000), AvrPphB (Nimchuk *et al.*, 2000), HopF2 (Robert-Seilaniantz *et al.*, 2006), and HopZ1 (Lewis *et al.*, 2008). Mutation of the myristoylation sites within these T3Es abolishes their function. The AvrBs3 T3E family from phytopathogenic species of *Xanthomonas* are targeted to the nucleus where they act as transcription factors (Van den Ackerveken *et al.*, 1996, Yang & Gabriel, 1995, Yang *et al.*, 2000). To date, the only T3E demonstrated to localize to plant organelles is HopI1 from *P. syringae*, which targets and remodels chloroplasts (Jelenska *et al.*, 2007).

We have previously demonstrated that several DC3000 T3Es, including HopG1, are suppressors of ETI responses including the HR (Jamir *et al.*, 2004). HopG1 was originally identified in a genome-wide screen for T3Es and was confirmed to be secreted in culture by DC3000 (Petnicki-Ocwieja *et al.*, 2002). The expression of HopG1 in yeast or tobacco can suppress cell death triggered by the pro-apoptotic mouse protein Bax (Jamir *et al.*, 2004), which is consistent with HopG1 acting as an ETI suppressor. Additionally, HopG1 was shown to be capable of suppressing vascular restriction in infected leaves (Oh & Collmer, 2005).

Communicated herein are additional functional analyses on HopG1 that provide insight on how it suppresses PCD and other innate immune responses. We demonstrate that *hopG1* is expressed in conditions that induce type III secretion and that a HopG1 protein fusion is injected into plant cells in a type III dependent manner. We show that HopG1 is capable of

suppressing PTI as well as ETI responses. Importantly, we show that HopG1 localizes to plant mitochondria suggesting that its targets in this organelle are involved in both PTI and ETI. Surprisingly, the constitutive expression of HopG1 *in planta* causes altered plant morphology and infertility possibly due to disruption of normal mitochondrial function by HopG1. We found that transgenic *A. thaliana* plants expressing HopG1 had reduced rates of respiration and enhanced basal levels of reactive oxygen species, further implying that mitochondrial function in these plants is impaired. Taken together these data suggest a broadly conserved pathogenic strategy where HopG1 suppresses host innate immunity by disrupting mitochondrial functions.

Results

HopG1 is a conserved protein found in several clades of bacteria

T3Es with high similarity to HopG1 are found in several T3SS-containing phytobacteria (Fig. S1). The percent protein identities as determined by pairwise BLAST of HopG1 from DC3000 with proteins that share similarity to HopG1 are as follows: *P. syringae* pv. *phaseolicola* 1448A, (53%); *Ralstonia solanacearum* GMI1000, (52%); *Xanthomonas axonopodis* pv. *citri*, (46%); *X. campestris* pv. *campestris* ATCC 33913, (48%); *Acidovorax avenae* subsp. *citrulli* AAC00-1, (46%) and *Rhizobium etli* CFN 42, (46%). We identified a putative cyclophilin binding site motif (GPxL) in the C-terminal half of these proteins (Fig. S1). This motif is found in the *P. syringae* T3E AvrRpt2, where it was shown to be necessary for the binding of a *A. thaliana* cyclophilin, a prerequisite for the proper folding and activity of AvrRpt2 (Coaker *et al.*, 2006). Bioinformatic analyses of HopG1's peptide sequence did not reveal additional insights as to its function or cellular target(s). However, the evolutionary conservation of HopG1-like T3Es across a range of plant-associated bacteria suggests that they have an important function in different types of bacterial-plant interactions.

DC3000 *hopG1* expression is enhanced in type III-inducing conditions and HopG1 is injected into plant cells

Bioinformatic analysis of DC3000 identified a putative Hrp box upstream of *hopG1*. Hrp boxes are binding sites for the alternative sigma factor HrpL that regulates the expression of genes under T3SS-inducing conditions (Xiao & Hutcheson, 1994). To experimentally demonstrate if *hopG1* is expressed under T3SS-inducing conditions, we isolated DC3000 RNA from cultures grown under T3SS-inducing and non-inducing conditions and performed semi-quantitative RT-PCR. These experiments showed that *hopG1* expression was increased in T3SS-inducing conditions in a manner similar to *hrpL* (Fig. 1A).

To determine if HopG1 is translocated into plant cells by the T3SS we used an adenylate cyclase (CyaA) fusion assay (Sory *et al.*, 1995). This assay determines if a protein can be injected into the plant cell as CyaA is dependent upon calmodulin for its activity and produces measurable levels of cAMP only when it is inside the plant cell but not when it is in the bacterial cell or plant apoplast. The presence of cAMP was detected in tobacco leaves infiltrated with DC3000 expressing HopG1-CyaA but not with the DC3000 T3SS defective *hrcC* mutant expressing HopG1-CyaA (Fig. 1B). These data confirm that HopG1-CyaA is translocated into plant cells by the T3SS of DC3000. The expression pattern, secretion (Petnicki-Ocwieja *et al.*, 2002), and translocation of HopG1 are all hallmarks of a T3E.

To determine if HopG1 contributes to virulence we performed *in planta* growth assays with UNL124, a DC3000 *hopG1* mutant (Jamir *et al.*, 2004). We spray-inoculated *A. thaliana* Col-0 with wild type DC3000 and the UNL124 strain and compared their growth. The UNL124 strain was not compromised in its virulence (Fig. S2). However, because DC3000

possesses greater than thirty T3Es HopG1's contribution to virulence may be masked by other T3Es that are functionally redundant.

Constitutive expression of HopG1 in plants alters development

To investigate the function of HopG1 *in planta* we made transgenic *A. thaliana* Col-0 plants that constitutively express a C-terminal hemagglutinin (HA) epitope-tagged HopG1 (HopG1-HA) using *Agrobacterium*-mediated transformation (Bechtold *et al.*, 1993). Expression of the epitope fused HopG1 product was confirmed in *A. thaliana* Col-0 primary transformants by immunoblotting using anti-HA antibodies (Fig S3). The *A. thaliana* Col-0 primary transformants expressing HopG1-HA were severely dwarf, highly branched and infertile (Fig. 2C and E). They also had a larger number of leaves and inflorescences (Fig. 2A) as well as increased root mass (Fig. 2E) when compared to wild type *A. thaliana* Col-0 (Fig. 2A, B and D). Importantly, these phenotypes were also observed in *Nicotiana tabacum* cv. Xanthi (tobacco) (Fig. 2G) and *Lycopersicon esculentum* cv. Moneymaker (tomato) (Fig. 2I) transgenic events constitutively expressing the HopG1-HA fusion protein. These data demonstrate that HopG1 expression *in planta* drastically impacts growth and development in members of the Solanaceae and Brassicaceae. These physiological changes are not seen in wild type plants infected with DC3000. They may reflect the consequences of constitutively expressed HopG1-HA interacting with its targets in cell types that otherwise would not be presented with this T3E during the course of bacterial/host interaction. Thus, it suggests that HopG1's virulence targets may also play a role, either directly or indirectly, in plant development.

HopG1 is a suppressor of plant innate immunity

HopG1 is a suppressor of ETI, as demonstrated by a DC3000 *hopG1* mutant eliciting an enhanced HR in tobacco (Jamir *et al.*, 2004) and was capable of suppressing an ETI-induced HR (Guo *et al.*, 2009). To determine the extent that HopG1 could also suppress PTI responses, *A. thaliana* Col-0 plants constitutively expressing HopG1-HA were spray-inoculated with a DC3000 T3SS defective *hrcC* mutant. Due to this mutant's inability to inject T3Es, PAMP recognition by the plant results in PTI, making this strain a de facto PTI inducer. The HopG1-HA-expressing plants accumulated higher titers of the *hrcC* mutant than wild type plants. A similar assay with wild type DC3000 showed that it grew similarly in HopG1-HA-expressing plants and in wild type plants (Fig. 3A). Taken together, these data indicate that HopG1 can suppress PTI.

To further examine the ability of HopG1 to suppress PTI the deposition of callose (β -1,3 glucan), an output of PTI, was monitored (Felix *et al.*, 1999). HopG1's impact on callose deposition was ascertained using two complementary approaches. Firstly, the peptide Flg21 was infiltrated into wild type *A. thaliana* Col-0 plants and plants expressing HopG1-HA. Flg21 is a conserved peptide of flagellin, which induces PTI responses due to its recognition by the PAMP receptor FLS2 (Gomez-Gomez & Boller, 2000). Callose deposits were visualized by staining with the fluorescent dye aniline blue. *A. thaliana* Col-0 plants expressing HopG1-HA had less foci stained with aniline blue than wild type Col-0 plants indicating that *in planta* expression of HopG1-HA suppressed callose deposition (Fig. 3B).

The second approach determined whether bacterial-delivered HopG1-HA could suppress callose deposition. The nonpathogen *P. fluorescens* (*Pf*) carrying construct pLN1965 (Wei *et al.*, 2007, Guo *et al.*, 2009), which expresses a functional T3SS from *P. syringae* pv. *syringae* 61. *Pf*(pLN1965) can inject an introduced T3E and allows the investigation of the biological activity of an individual T3E. Importantly, *Pf*(pLN1965) also induces PTI (including callose deposition) due to the presence of PAMPs found in *P. fluorescens* that are recognized by plants. An empty vector control or a construct carrying *hopG1-ha* were

introduced into *Pf*(pLN1965). The resultant strains were infiltrated at a cell density of 1×10^6 cells/ml into wild type *A. thaliana* Col-0 plants and callose deposition was measured. Indeed, callose deposition in plants infiltrated with *Pf*(pLN1965) expressing HopG1-HA was reduced compared to those infiltrated with an empty vector control (Fig. 3B). Taken together, both experimental approaches demonstrate that HopG1 can suppress PTI. Moreover, since HopG1 can also suppress ETI it suggests that HopG1 may target components of plant immunity common to both responses.

To determine the extent that HopG1 could suppress specific PTI-induced genes we examined the expression of PR1 and WRKY22 in wild type and HopG1-HA-expressing *A. thaliana* treated with Flg21 (Fig. 3C). This was accomplished using semi-quantitative RT-PCR. Both PR1 and WRKY22 have been shown to be induced in response to flagellin (Gomez-Gomez *et al.*, 1999, Navarro *et al.*, 2004). We found that Flg21-induced expression of both PR1 and WRKY22 was reduced in HopG1-HA expressing plants. These data further confirm that HopG1 can suppress PTI.

HopG1 is targeted to plant mitochondria

The subcellular localization of a T3E can provide clues to its function. With this in mind we investigated the subcellular targeting of HopG1. To this end, a *hopG1* gene fusion that when expressed would link the C-terminus of the protein to the green fluorescence protein (GFP) was assembled and cloned into a binary vector downstream of a constitutive 35S CaMV promoter. The resultant construct was introduced into *Agrobacterium* and the derived strain infiltrated into tobacco leaves. After 48 hours the infiltrated leaves were viewed with confocal microscopy. HopG1-GFP was localized to small discrete points in the cytosol (Fig. 4A). The punctate fluorescence pattern was reminiscent of those produced by mitochondrially-targeted GFP fusions (Forner & Binder, 2007).

To determine if HopG1-GFP was indeed localized to mitochondria we performed co-localization experiments with HopG1-GFP and an N-terminal mitochondrial targeting sequence from isovaleryl-CoA-dehydrogenase (IVD) fused to the red fluorescent protein eqFP611 (Forner & Binder, 2007). The nucleotide sequence corresponding to the IVD-eqFP611 was sub-cloned into the pZP212 binary vector. *Agrobacterium* strains carrying HopG1-GFP or IVD-eqFP611 constructs were mixed and infiltrated into tobacco leaves. After 48 hours infiltrated leaves were viewed with confocal microscopy. Plant cells expressing both HopG1-GFP and IVD-eqFP611 produced punctate yellow spots in their cytoplasm indicating that HopG1-GFP co-localized with IVD-eqFP611 and is, therefore, targeted to the mitochondria (Fig. 4A).

To confirm localization to the mitochondria intact organelles were isolated from wild type and HopG1-HA expressing tobacco leaves using Percoll density gradient fractionation. Levels of HopG1-HA in mitochondria fractions were compared to those in total protein extracts with immunoblots using anti-HA antibodies. Enrichment of HopG1-HA was observed in the mitochondrial fraction of HopG1-HA expressing tobacco indicating organellar localization (Fig. 4B). Control immunoblots using antibodies to alternative oxidase (AOX), a known mitochondrial protein, were performed to confirm that there was an enrichment of mitochondrial proteins in the mitochondria fractions when compared to total protein extracts. These subcellular fractionation experiments confirm that HopG1-HA is localized to the mitochondria.

To determine if the putative T3Es that share high similarity to HopG1 also localize to the mitochondria we repeated the confocal microscopy experiments with a HopG1 homolog from *X. campestris* pv. *campestris* ATCC 33913, HopG1_{Xcc} (NP_638946), which is 48% identical to HopG1 (Fig. S1). A HopG1_{Xcc}-GFP fusion construct was introduced into

Agrobacterium and infiltrated into tobacco leaves. The HopG1_{Xcc}-GFP fusion also localized to the mitochondria as supported by the observed co-localization with IVD-eqFP611 (Fig. S4). These data indicate that the putative T3Es that share similarity with HopG1 also localize to the mitochondria and suggest that this localization is vital for their function.

The mitochondrial targeting sequence is in the N-terminus of HopG1

A conserved mitochondrial targeting sequence was not identified within the 492 amino acid long HopG1 protein using bioinformatics tools. To define a region within HopG1 that is required for mitochondrial targeting we made truncated versions of HopG1 fused C-terminally to GFP. These proteins were transiently expressed in tobacco and subsequently imaged using confocal microscopy. The N-terminal regions spanning amino acids 1–263 or 1–380 of HopG1 fused to GFP displayed mitochondrial localization indicating that the N-terminal 263 amino acids of HopG1 are sufficient for mitochondrial targeting (Fig. 5A and B). HopG1 regions encompassing amino acids 1–160, 14–492, 100–200, 160–492 or 263–492 fused to GFP localized to the cytoplasm and nucleus in a manner similar to that of the GFP control (Fig. 5A and B). The expression and size of all fusion proteins were confirmed with protein blots using anti-GFP antibodies (data not shown). Note that the chloroplasts in some images appear yellow due to the low level of accumulation of full length HopG1-GFP that necessitated the use of detection conditions for GFP that also detected chlorophyll autofluorescence. In addition, a site-directed mutant in the putative cyclophilin binding site (Fig. S1) of HopG1-GFP that has an alanine in position 350 of the peptide instead of a glycine (HopG1_{G350A}-GFP) retained its ability to target the mitochondria (Fig. 5A and B). This suggests that cyclophilin binding is not required for the production of HopG1 *in planta* or its mitochondrial localization.

Combined these data indicate that the mitochondrial targeting signal of HopG1 is within its N-terminal 263 amino acids. Moreover, the failure of the HopG1-GFP fusion lacking the N-terminal 13 amino acids to be targeted to the mitochondria clearly shows that the N-terminus of HopG1 is important for mitochondrial localization (Fig. 5A and B). Consistent with this, an N-terminal GFP fusion to full-length HopG1 also localized to the cytoplasm and nucleus suggesting that mitochondrial localization requires a free HopG1 N-terminus (data not shown). These data suggest that regions in the first 263 amino acids as well as a free HopG1 N-terminus are necessary for mitochondrial localization.

HopG1-GFP truncations do not alter plant development

To test the hypothesis that mitochondrial localization is important for the function of HopG1 we determined which regions of HopG1 were necessary to cause the altered plant development observed in transgenic plants constitutively expressing HopG1-HA (Fig. 2). To accomplish this constructs corresponding to full length HopG1-GFP, and the respective HopG1-GFP fusions described above, along with the HopG1_{G350A}-GFP amino acid substitution derivative were stably transformed into *A. thaliana* Col-0 plants via *Agrobacterium*-mediated transformation. The resulting seeds for each transgenic plant were germinated on selective medium and acclimated to soil. Expression of the HopG1-GFP derivatives was confirmed by immunoblot analysis with anti-GFP antibodies (data not shown). The derived transgenic events were assessed for the HopG1-induced developmental phenotype. Transgenic plants constitutively expressing full length HopG1-GFP produced the same developmental phenotype as those expressing HopG1-HA (Fig. 5A and C). All plants expressing HopG1-GFP truncations resembled wild type *A. thaliana* Col-0 indicating that HopG1 derivatives were no longer capable of inducing this phenotype (Fig. 5A and C). Importantly, the HopG1-GFP truncations that did not localize to the mitochondria did not produce the plant phenotype. On the other hand, HopG1_{G350A}-GFP went to the mitochondria and produced the HopG1-induced developmental phenotype. Particularly

noteworthy is that the developmental phenotype is not induced by HopG1₁₄₋₄₉₂-GFP that lacks only the N-terminal 13 amino acids of HopG1 and does not localize to the mitochondria (Fig. 5). We also determined if the mitochondrial targeting of HopG1 was necessary for the ability of HopG1 to suppress PTI. To accomplish this, the deposition of Flg21 induced callose in transgenic *A. thaliana* expressing HopG1 truncations fused to GFP was examined. When compared to plants expressing GFP alone, plants expressing HopG1-GFP had 47±5 % less callose and plants expressing HopG1_{G350A}-GFP had 68±4 % less callose. In contrast, plants expressing HopG1₁₋₃₈₀-GFP or HopG1₁₆₀₋₄₉₂-GFP displayed similar callose deposition to plants expressing GFP alone, 5±7 % less and 20±10 % more, respectively.. These results suggest that both mitochondrial targeting and an activity in the C-terminus of HopG1 are required for HopG1's activity.

HopG1 alters respiration and ROS accumulation

The localization of HopG1 to plant mitochondria implies that mitochondria are involved in HopG1's ability to suppress innate immunity. HopG1 may suppress innate immunity by altering mitochondrial functions, such as the rate of respiration. Therefore, we determined if HopG1-HA altered basal respiration by measuring the rate of oxygen consumption of leaf disks of wild type and HopG1-HA-expressing tobacco in the dark. The rate of oxygen consumption of tobacco expressing HopG1-HA was approximately half that of wild type tobacco (Fig. 6A) suggesting that HopG1 impairs mitochondrial respiration and thus may cause mitochondrial dysfunction.

Restriction of mitochondrial respiration can lead to an increased production of reactive oxygen species (ROS) (Maxwell *et al.*, 1999). To determine if this is the case in HopG1-HA-expressing tobacco we compared its steady state ROS levels to those of wild type tobacco. Relative ROS levels were determined using the ROS-sensitive fluorescent probe 2',7'-dichlorodihydrofluorescein (H2DCFHDA). Tobacco plants expressing HopG1-HA produced approximately four fold higher basal levels of ROS than wild type tobacco plants (Fig. 6B). These data show that the expression of HopG1-HA does result in increased ROS production in tobacco. These enhanced ROS levels may be due to altered mitochondrial functions in HopG1-HA-expressing plants.

Discussion

In this study we show that the DC3000 *hopG1* gene is expressed under T3SS-inducing conditions and a HopG1-CyaA fusion is injected into plant cells (Fig. 1). This confirms an earlier report using a different translocation assay, that HopG1 is translocated (Petnicki-Ocwieja *et al.*, 2002). A DC3000 mutant lacking HopG1 was not detectably reduced in virulence compared to wild type DC3000 (Fig. S2). We have previously reported that HopG1 can suppress ETI (Jamir *et al.*, 2004, Guo *et al.*, 2009). We extended this finding here by showing that HopG1 can also suppress PTI (Fig. 3). Thus, HopG1 is a suppressor of both the PTI and ETI branches of plant innate immunity. Given this significant activity it seems likely that the lack of a virulence phenotype for the DC3000 *hopG1* mutant is due to the presence of other functionally redundant T3Es. Several *P. syringae* T3Es have now been characterized for their ability to suppress PTI or ETI. An emerging theme appears to be that many T3Es can suppress both immunity branches. Perhaps this is reasonable to expect since many T3Es have multiple activities and that ETI and PTI share many of their signaling components and response outputs (Tao *et al.*, 2003, Navarro *et al.*, 2004).

The HopG1-induced plant developmental phenotype observed in transgenic *A. thaliana*, tomato, and tobacco (Fig. 2) is intriguing and warrants further discussion. We view phenotypes caused by the transgenic expression of T3Es as potential clues to their activities because they may be caused by the enzymatic activity of the T3E or be due to the effect the

T3E has on a plant target or targets. The fact that we were unable to separate the plant phenotype induced by HopG1 from the localization of HopG1 to mitochondria suggests that the phenotype is associated with the site of action of HopG1 and not simply due to nonspecific activity. Moreover, alterations in plant development can be associated with impaired mitochondrial function. This is particularly true for defects in fertility such as cytoplasmic male sterility but occasionally alterations in plant growth rates and architecture are also observed (Shedge *et al.*, 2007). However, we cannot at this point be certain that the HopG1-induced developmental phenotype is connected to HopG1's virulence role. One possibility that we are currently exploring is whether HopG1 modulates plant hormone levels. Many different hormones control plant growth and/or biotic stress responses. These hormones include ABA, ethylene, jasmonic acid, brassinosteroids, gibberellins, auxins and SA. They work in complex and finely balanced networks which several T3Es and toxins have been shown to disrupt to the advantage of the pathogen. See (Grant & Jones, 2009, Pieterse *et al.*, 2009, Santner *et al.*, 2009) for recent reviews on these networks. It is quite possible, perhaps even likely, that the modified developmental phenotype of HopG1-expressing plants is due to an effect on one or more of these networks.

To our knowledge HopG1 is the first plant pathogen T3E shown to localize to plant mitochondria. HopG1 lacks a predictable mitochondrial targeting sequence, however, our studies here showed that amino acids 1–263 of HopG1 were sufficient for localization to the mitochondria (Fig. 5). Neither amino acids 1–160, 14–492, 100–200 nor 160–492 of HopG1 were sufficient for mitochondrial localization suggesting that a fairly large portion of the protein is required for mitochondrial targeting. This targeting could occur directly or be due to the interaction of HopG1 with a host protein that is targeted to the mitochondria. Mitochondrial targeting without a predictable targeting sequence is not uncommon as several bacterial pathogenicity factors imported into animal mitochondria do not have these targeting sequences (Kozjak-Pavlovic *et al.*, 2008).

Our bioinformatic analyses identified a putative cyclophilin binding site in HopG1. These sites have been found in the *P. syringae* T3E AvrRpt2, where they are required for this effector to be processed *in planta* and for its cysteine protease activity (Coaker *et al.*, 2005, Coaker *et al.*, 2006). The putative cyclophilin binding site present in HopG1 was not required for the HopG1-induced plant phenotype or mitochondrial localization. However, it is possible that our assays may not have detected a reduction in properly folded HopG1 as long as there was enough to detect its localization to mitochondria and to cause the associated phenotype.

To determine if HopG1 can alter mitochondrial function we measured the effect of HopG1 on respiration a common marker of altered mitochondria function. We demonstrated that the expression of HopG1-HA in tobacco leaves leads to a decrease in the rate of oxygen consumption coupled with enhanced basal levels of ROS. These data are consistent with the hypothesis that HopG1 alters mitochondrial function although they cannot rule out that the alteration of respiration is a secondary effect in the HopG1-HA-expressing plants. Additional experiments are required to determine the exact site and immediate consequences of HopG1 action.

Mitochondria are also involved in plant innate immunity signaling pathways (Maxwell *et al.*, 2002). Thus, HopG1's ability to suppress plant innate immunity may be due to its ability to alter mitochondrial function. One possible outcome of HopG1's interaction with mitochondria is PCD suppression. PCD is a common response to pathogen infection for both resistant and susceptible hosts (Greenberg & Yao, 2004) and mitochondria play a major role in regulating it (Lam *et al.*, 2001). There is a precedent for T3Es acting to alter PCD responses at the mitochondrial level. For example, bacterial pathogens of animals have been

shown to prevent apoptosis by activating cell survival signals, degrading pro-apoptotic proteins, and protecting mitochondria (see (Faherty & Maurelli, 2008) for a recent review). We have previously shown that HopG1 can suppress the HR and prevent Bax-induced cell death in yeast and tobacco (Jamir et al., 2004). Bax is thought to initiate PCD by interacting with mitochondria to cause the release of pro-apoptotic factors (Jurgensmeier *et al.*, 1998). Our current data indicate that HopG1 localizes to the mitochondria and suppresses plant innate immunity. Thus, it is possible that HopG1 does so by directly protecting mitochondria from the action or release of pro-apoptotic factors.

Other plant pathogens have T3Es that have high identity to HopG1 suggesting that these are broadly important T3Es. At least one of these is also localized to the mitochondria (Fig. S4). Thus, our findings reveal a novel site of action for a plant pathogen T3E and suggest that plant pathogens target mitochondria to disable plant immunity.

Experimental procedures

RT-PCR analysis

DC3000 strains were grown in King's B (KB) broth (King *et al.*, 1954) and T3SS-inducing minimal media (Yuan & He, 1996) with the appropriate antibiotics at 22°C for 3 hours and the cells were harvested at log phase. Transgenic *A. thaliana* plants were infiltrated with 10µM Flg21 and tissue was harvested 16h later. Total RNA was purified using RNeasy® mini Kit (QIAGEN, www.qiagen.com). Extensive DNase treatment of the RNA was performed with DNA-free® (Ambion, www.ambion.com). The reverse transcription of RNA was carried out using RETROscript® (Ambion, www.ambion.com) using oligo (dT) primers with heat denaturation of the RNA. *hopG1* was amplified using primers 5'-CACCATGCAAATAAAGAACAGTCATCTC-3' (P2887) and 5'-GCCGTTGTAATAACTGCTTAGAGG-3' (P2890). *hrpL* was amplified using primers 5'-AGTGAATTCATGTTTCAGAAGATTGTG-3' (P1626) and 5'-AGTCTCGAGTCAGGCCGACGGGTCGAT-3' (P1627). PCR conditions were 30 cycles of 94°C for 30 sec, 50°C for 30 sec and 72°C for 1.5 min followed by an extension of 72°C for 10 min. *Actin* was amplified using primers 5'-CTAAGCTCTCAAGATCAAAGGC-3' (P2228) and 5'-TTAACATTGCAAAGAGTTTCAAGG-3' (P2229). *PR1* was amplified using primers 5'-TGAATTTTACTGGCTATTCTCG-3' (P1268) and 5'-TCTCAAACAACCTGAGTGT-3' (P1269). WRKY22 was amplified using primers 5'-CACCAACAATGGCCGACGATTGGGATCTC-3' (P1475) and 5'-TATTCCTCCGGTGGTAGTG-3' (P1476). PCR conditions were 30 cycles of 94°C for 10 sec, 52°C for 30 sec and 72°C for 30 sec followed by an extension of 72°C for 5 min.

Adenylate cyclase (CyaA) translocation assay

A construct encoding a HopG1 C-terminal CyaA fusion was made by the recombination of pENTR/D-TOPO::*hopG1* with the Gateway vector pLN2193 (Fu *et al.*, 2006). It was then transformed into DC3000 and *hrcC* strains by electroporation. The CyaA assays were performed following a previously described protocol (Schechter *et al.*, 2004). Briefly, freshly grown bacteria from plates were suspended in 5 mM morpholinoethanesulfonic acid (MES), pH5.6, at OD₆₀₀ of 0.5. Then the bacterial suspensions were infiltrated into *N. benthamiana* leaves. Leaf disks of 0.9 cm in diameter were harvested 7 hours after infiltration and ground in liquid nitrogen and resuspended in 0.1 M HCl. A direct cyclic AMP (cAMP) correlate enzyme immunoassay kit (Assay Designs, www.assaydesigns.com) was used to measure cAMP concentrations in each sample following the manufacturer's instructions.

Transgenic plant production

Transgenic plants constitutively expressing HopG1 were made by *Agrobacterium*-mediated plant transformation with pPZP212:*hopG1-HA* (pLN530) (Jamir et al., 2004) or the pK7FWG2:*hopG1* constructs. *A. thaliana* Col-0 plants were transformed by floral dip (Bechtold et al., 1993). Tobacco and tomato transformations were carried out as described (Horsch et al., 1985, McCormick et al., 1986). Experiments were performed at least twice with similar results using at least four primary transformants for each construct. Transgene accumulation was determined by Western blotting, RT-PCR and/or confocal microscopy.

A. *thaliana* pathogenicity assays

DC3000, the DC3000 *hopG1* mutant (UNL124) (Jamir et al., 2004), and the DC3000 *hrcC* mutant (Yuan & He, 1996) were grown overnight at 30°C on KB agar plates with the appropriate antibiotics and bacterial suspensions were made to an OD₆₀₀ of 0.2 in 10 mM MgCl₂ containing 0.02% (v/v) silwet (Lehle Seeds, www.arabidopsis.com). *A. thaliana* Col-0 plants grown for 4 weeks at 25°C on 10 hour days were covered with a humidity dome overnight and then sprayed with a fine mist of the bacterial suspension. 1 cm² leaf disks were sampled from the infected tissue and ground in 10 mM MgCl₂. The plating of serial dilutions of the samples on KB agar with the appropriate antibiotics allowed the number of colony forming units (cfu) of DC3000 in the leaf tissue to be determined. ANOVA was performed for all appropriate experiments.

Callose deposition assay

For assaying Flg21-induced callose deposition, wild type *A. thaliana* Col-0, HopG1-HA, HopG1-GFP and HopG1-GFP truncation transgenic plants were infiltrated with 10 μM Flg21. For assaying callose deposition induced by *P. fluorescens* (*Pf*), wild type *A. thaliana* Col-0 was infiltrated with 10⁸ cells/ml of *Pf*(pLN1965) carrying pML123 or pML123:*hopG1-HA*. Sixteen hours after infiltration leaf samples were cleared with alcoholic lactophenol, rinsed with 50% ethanol (v/v) followed by water as described (Adam & Somerville, 1996). The completely cleared leaves were stained with 0.01% aniline blue (w/v) in a solution of 150 mM K₂HPO₄, pH 9.5, for 30 min. The callose deposits were visualized with a Zeiss Axionplan 2 imaging Microscope. QUANTITY ONE software (Bio-Rad, www.bio-rad.com) was used to enumerate callose deposits.

HopG1 immunofluorescence assays

HopG1 truncated constructs were made by amplifying *hopG1* from DC3000 total DNA by PCR with Pfu polymerase using 30 cycles of 94°C for 1 min, 52°C for 1 min and 72°C for 1.5 min followed by an extension of 72°C for 10 min. The following primers were used for the gene truncations and the corresponding amino acid location of the primer and its primer number are in the parenthesis: 5'-CACCATGCAAATAAAGAACAGTCATCTC-3' (HopG1₁, P2887), 5'-CACCTCGAGATGGTGCAGAATACTTTAATG-3' (HopG1₁₄, P3498), 5'-CACCATGGGTGGTTTTACCAGCGATGCCAGG-3' (HopG1₁₀₀, 3014), 5'-CACCATGTCCGACCTAGTTGACACGG AGC-3' (HopG1₁₆₀, P3015), 5'-CACCATGGAAACTCTTGATAACTTACTTCG-3' (HopG1₂₆₃, P2889), 5'-GGAGAGGTAAATCTTAGTTGC-3' (HopG1₁₆₀, P2964), 5'-GTCTTTTGGTGTTTTTTCCGGGT-3' (HopG1₂₀₀, P2965), 5'-CATTGATTTATGTTTCAAATCTTCTATTTT -3' (HopG1₂₆₃, P2888), 5'-CATTGATTTATGTTTCAAATCTTCTATTTT-3' (HopG1₃₈₀, P2886), and 5'-GCCGTTGTAAACTGCTTAGAGG -3' (HopG1₄₉₂, P2890). PCR products were placed into pENTR/D-TOPO (Invitrogen, www.invitrogen.com) and then recombined into pK7FWG2 (Karimi et al., 2002) to create constructs that express C-terminal GFP fusion proteins. These were then transiently expressed in tobacco leaves by *Agrobacterium*-

mediated transformation (Jamir et al., 2004). Localization of GFP fusions were visualized with sequential laser scanning confocal microscopy using an Olympus FV500 with sequential imaging at 488 nm excitation and 505–525 nm emission, (green/GFP) and 633 nm excitation and 660 nm emission (red/chlorophyll). The HopG1_{G350A} cyclophilin binding site mutant was made by using the QuickChange™ site-directed mutagenesis kit (Stratagene, www.stratagene.com) to change the codon GGG to GCC on pENTR/D-TOPO::hopG1_{1–492} with the primers 5'-GGAATACCAGCATTGCAGCCCCAGTGCTCTACCACGC-3' (P3008) and 5'-GCGTGGTAGAGCACTGGGGCTGCAATGCTGGTATTCC-3' (P3009). Co-localization with mitochondria was performed with pIVD-eqFP611 (Forner & Binder, 2007) that was cloned in a Gateway version of pPZP212 using the primers IVDfw: 5'-CACCATGCAGAGGTTTTTCTCCGC-3' (P3415) and eqFP611rev: 5'-TCAAAGACGTCCCAGTTTGG-3' (P3040) for *Agrobacterium*-mediated transformation. Laser scanning confocal microscopy with 543 nm excitation and 560–600 nm emission wavelengths was used to visualize the IVD-eqFP611 fusion protein.

Subcellular fractionation

Fifty g of tobacco leaf tissue was shredded and gently disrupted with a mortar and pestle in 120 ml of extraction medium (EM) (20 mM HEPES-Tris, pH 7.6, 0.4 M sucrose, 5 mM EDTA, 0.6% PVP (w/v), 0.6 mM cysteine). The extract was filtered through 8 layers of cheesecloth and centrifuged 5 min at 3500 g. The supernatant was centrifuged at 28,000 g for 10 min to pellet organelles. The pellet was resuspended in 120 ml EM without PVP and centrifuged at 28,000 g for 10 min and the pellet resuspended in 2 ml of suspension buffer (SB) (10 mM MOPS-KOH, pH 7.2, 0.2 M sucrose) and loaded on a Percoll gradient of 10%, 32% and 50% percoll in SB. The gradient was centrifuged at 40,000 g and the mitochondria collected as a band between the 32% and 50% percoll stages. The mitochondrial fraction was washed three times in two volumes of SB by centrifugation at 16,000 g for 40 min. Protein blots were performed with anti-HA antibodies (Roche, www.roche.com) and anti-AOX antibodies (Elthon *et al.*, 1989).

Oxygen consumption

1 cm² leaf disks were cut from wild type tobacco and tobacco constitutively expressing HopG1-HA. Oxygen consumption was measured polarographically using a Rank Brothers oxygen electrode (Rank Brothers Ltd. www.rankbrothers.co.uk) at 25°C in 1 ml of air-saturated water in the dark. Each experiment was done with three replicates.

ROS measurement

Leaf tissue from wild type tobacco and tobacco constitutively expressing HopG1-HA was ground in liquid nitrogen and resuspended in ice cold 10 mM Tris-HCl, pH 7.3. Samples were centrifuged twice to remove cell debris and 0.1 ml of the supernatant was placed in duplicate on a Microfluor®1 white wellplate (Thermo Scientific, www.thermofisher.com). 2'-7'-dichlorodihydrofluorescein diacetate (H2DCFDA, Invitrogen, www.Invitrogen.com) to a final concentration of 10 µM was added to the wells and mixed. Fluorescence was measured with an excitation wavelength of 485 nm and an emission wavelength of 535 nm on a CaryEclipse fluorometer. Protein content was determined by the Bradford assay and relative basal ROS levels calculated with wild type tobacco set to 1.

Supplementary Material

Refer to Web version on PubMed Central for supplementary material.

Acknowledgments

We thank members of the Alfano laboratory for many fruitful discussions regarding HopG1 and in particular Matt Dale for his assistance with experiments. We thank Thomas Elthon for the anti-AOX antibodies, Stefan Binder for IVD-eqFP611 and Fang Tian for the CyaA assays. We also thank Thomas Elthon and Sally Mackenzie for advice about our experiments with plant mitochondria. This research was supported by grants from the National Science Foundation (Award No. MCB-0544447), United States Department of Agriculture (2007-35319-18336), and the National Institutes of Health (Award No. 1R01AI069146-01A2) and funds from the Center for Plant Science Innovation at the University of Nebraska.

References

- Abramovitch RB, Anderson JC, Martin GB. Bacterial elicitation and evasion of plant innate immunity. *Nat. Rev. Mol. Cell Biol.* 2006; 7:601–611. [PubMed: 16936700]
- Abramovitch RB, Kim YJ, Chen S, Dickman MB, Martin GB. *Pseudomonas* type III effector AvrPtoB induces plant disease susceptibility by inhibition of host programmed cell death. *EMBO.* 2003; 22:60–69.
- Adam L, Somerville SC. Genetic characterization of five powdery mildew disease resistance loci in *Arabidopsis thaliana*. *Plant J.* 1996; 9:341–356. [PubMed: 8919911]
- Alfano JR, Charkowski AO, Deng W, Badel JL, Petnicki-Ocwieja T, van Dijk K, Collmer A. The *Pseudomonas syringae* Hrp pathogenicity island has a tripartite mosaic structure composed of a cluster of type III secretion genes bounded by exchangeable effector and conserved effector loci that contribute to parasitic fitness and pathogenicity in plants. *Proc. Natl. Acad. Sci. USA.* 2000; 97:4856–4861. [PubMed: 10781092]
- Alfano JR, Collmer A. Type III secretion system effector proteins: Double agents in bacterial disease and plant defense. *Annu. Rev. Phytopathol.* 2004; 42:385–414. [PubMed: 15283671]
- Ausubel FM. Are innate immune signaling pathways in plants and animals conserved? *Nat. Immunol.* 2005; 6:973–979. [PubMed: 16177805]
- Bechtold N, Ellis J, Pelletier G. In planta *Agrobacterium* mediated gene transfer by infiltration of adult *Arabidopsis thaliana* plants. *C. R. Acad. Sci. Paris.* 1993; 316:1194–1199.
- Block A, Li G, Fu ZQ, Alfano JR. Phytopathogen type III effector weaponry and their plant targets. *Curr. Opin. Plant Biol.* 2008; 11:396–403. [PubMed: 18657470]
- Chisholm ST, Coaker G, Day B, Staskawicz BJ. Host-microbe interactions: shaping the evolution of the plant immune response. *Cell.* 2006; 124:803–814. [PubMed: 16497589]
- Coaker G, Falick A, Staskawicz B. Activation of a Phytopathogenic Bacterial Effector Protein by a Eukaryotic Cyclophilin. *Science.* 2005; 308:548–550. [PubMed: 15746386]
- Coaker G, Zhu G, Ding Z, Van Doren SR, Staskawicz B. Eukaryotic cyclophilin as a molecular switch for effector activation. *Mol Microbiol.* 2006; 61:1485–1496. [PubMed: 16968222]
- Cunnac S, Lindeberg M, Collmer A. *Pseudomonas syringae* type III secretion system effectors: repertoires in search of functions. *Curr. Opin. Microbiol.* 2009; 12:53–60. [PubMed: 19168384]
- Elthon TE, Nickels RL, McIntosh L. Monoclonal Antibodies to the Alternative Oxidase of Higher Plant Mitochondria. *Plant Physiol.* 1989; 89:1311–1317. [PubMed: 16666702]
- Espinosa A, Alfano JR. Disabling surveillance: bacterial type III secretion system effectors that suppress innate immunity. *Cell. Microbiol.* 2004; 6:1027–1040. [PubMed: 15469432]
- Faherty CS, Maurelli AT. Staying alive: bacterial inhibition of apoptosis during infection. *Trends Microbiol.* 2008; 16:173–180. [PubMed: 18353648]
- Felix G, Duran JD, Volko S, Boller T. Plants have a sensitive perception system for the most conserved domain of bacterial flagellin. *Plant J.* 1999; 18:265–276. [PubMed: 10377992]
- Forner J, Binder S. The red fluorescent protein eqFP611: application in subcellular localization studies in higher plants. *BMC plant biology.* 2007; 7:28. [PubMed: 17553146]
- Fu ZQ, Guo M, Alfano JR. *Pseudomonas syringae* HrpJ is a type III secreted protein that is required for plant pathogenesis, injection of effectors, and secretion of the HrpZ1 harpin. *J. Bacteriol.* 2006; 188:6060–6069. [PubMed: 16923873]
- Gomez-Gomez L, Boller T. FLS2: an LRR receptor-like kinase involved in the perception of the bacterial elicitor flagellin in *Arabidopsis*. *Mol. Cell.* 2000; 5:1003–1011. [PubMed: 10911994]

- Gomez-Gomez L, Felix G, Boller T. A single locus determines sensitivity to bacterial flagellin in *Arabidopsis thaliana*. *Plant J.* 1999; 18:277–284. [PubMed: 10377993]
- Grant MR, Jones JD. Hormone (dis)harmony moulds plant health and disease. *Science.* 2009; 324:750–752. [PubMed: 19423816]
- Greenberg JT, Yao N. The role and regulation of programmed cell death in plant-pathogen interactions. *Cell Microbiol.* 2004; 6:201–211. [PubMed: 14764104]
- Guo M, Tian F, Wamboldt Y, Alfano JR. The majority of the type III effector inventory of *Pseudomonas syringae* pv. *tomato* DC3000 can suppress plant immunity. *Mol. Plant Microbe Interact.* 2009; 22:1069–1080. [PubMed: 19656042]
- Horsch RB, Fry JE, Hoffmann NL, Eichholtz D, Rogers SG, Fraley RT. A simple and general method for transferring genes into plants. *Science.* 1985; 227:1229–1231. [PubMed: 17757866]
- Jamir Y, Guo M, Oh H-S, Petnicki-Ocwieja T, Chen S, Tang X, Dickman MB, Collmer A, Alfano JR. Identification of *Pseudomonas syringae* type III effectors that suppress programmed cell death in plants and yeast. *Plant J.* 2004; 37:554–565. [PubMed: 14756767]
- Jelenska J, Yao N, Vinatzer BA, Wright CM, Brodsky JL, Greenberg JT. A J domain virulence effector of *Pseudomonas syringae* remodels host chloroplasts and suppresses defenses. *Curr Biol.* 2007; 17:499–508. [PubMed: 17350264]
- Jones JD, Dangl JL. The plant immune system. *Nature.* 2006; 444:323–329. [PubMed: 17108957]
- Jurgensmeier JM, Xie Z, Deveraux Q, Ellerby L, Bredesen D, Reed JC. Bax directly induces release of cytochrome *c* from isolated mitochondria. *Proc. Natl. Acad. Sci. USA.* 1998; 95:4997–5002. [PubMed: 9560217]
- Karimi M, Inze D, Depicker A. GATEWAY vectors for *Agrobacterium*-mediated plant transformation. *Trends Plant Sci.* 2002; 7:193–195. [PubMed: 11992820]
- King EO, Ward MK, Raney DE. Two simple media for the demonstration of pyocyanin and fluorescein. *J. Lab. Med.* 1954; 22:301–307.
- Kozjak-Pavlovic V, Ross K, Rudel T. Import of bacterial pathogenicity factors into mitochondria. *Curr. Opin. Microbiol.* 2008; 11:9–14. [PubMed: 18280201]
- Lam E, Kato N, Lawton M. Programmed cell death, mitochondria and the plant hypersensitive response. *Nature.* 2001; 411:848–853. [PubMed: 11459068]
- Lewis JD, Abada W, Ma W, Guttman DS, Desveaux D. The HopZ family of *Pseudomonas syringae* type III effectors require myristoylation for virulence and avirulence functions in *Arabidopsis thaliana*. *J. Bacteriol.* 2008; 190:2880–2891. [PubMed: 18263728]
- Lindeberg M, Cartinhour S, Myers CR, Schechter LM, Schneider DJ, Collmer A. Closing the circle on the discovery of genes encoding Hrp regulon members and type III secretion system effectors in the genomes of three model *Pseudomonas syringae* strains. *Mol. Plant Microbe Interact.* 2006; 19:1151–1158. [PubMed: 17073298]
- Maxwell DP, Nickels R, McIntosh L. Evidence of mitochondrial involvement in the transduction of signals required for the induction of genes associated with pathogen attack and senescence. *Plant J.* 2002; 29:269–279. [PubMed: 11844105]
- Maxwell DP, Wang Y, McIntosh L. The alternative oxidase lowers mitochondrial reactive oxygen production in plant cells. *Proc Natl Acad Sci U S A.* 1999; 96:8271–8276. [PubMed: 10393984]
- McCormick SM, Niedermeyer J, Fry J, Barnason A, Horsch R, R F. Leaf disc transformation of cultivated tomato (*L. esculentum*) using *Agrobacterium tumefaciens*. *Plant Cell Reports.* 1986; 5:81–84.
- Navarro L, Zipfel C, Rowland O, Keller I, Robatzek S, Boller T, Jones JD. The transcriptional innate immune response to flg22. Interplay and overlap with Avr gene-dependent defense responses and bacterial pathogenesis. *Plant Physiol.* 2004; 135:1–16.
- Nimchuk Z, Marois E, Kjemtrup S, Leister RT, Katagiri F, Dangl JL. Eukaryotic fatty acylation drives plasma membrane targeting and enhances function of several type III effector proteins from *Pseudomonas syringae*. *Cell.* 2000; 101:353–363. [PubMed: 10830163]
- Nurnberger T, Brunner F, Kemmerling B, Piater L. Innate immunity in plants and animals: striking similarities and obvious differences. *Immunol. Rev.* 2004; 198:249–266. [PubMed: 15199967]

- Oh HS, Collmer A. Basal resistance against bacteria in *Nicotiana benthamiana* leaves is accompanied by reduced vascular staining and suppressed by multiple *Pseudomonas syringae* type III secretion system effector proteins. *Plant J.* 2005; 44:348–359. [PubMed: 16212612]
- Petnicki-Ocwieja T, Schneider DJ, Tam VC, Chancey ST, Shan L, Jamir Y, Schechter LM, Janes MD, Buell CR, Tang X, Collmer A, Alfano JR. Genomewide identification of proteins secreted by the Hrp type III protein secretion system of *Pseudomonas syringae* pv. *tomato* DC3000. *Proc. Natl. Acad. Sci. USA.* 2002; 99:7652–7657. [PubMed: 12032338]
- Pieterse CM, Leon-Reyes A, Van der Ent S, Van Wees SC. Networking by small-molecule hormones in plant immunity. *Nat. Chem. Biol.* 2009; 5:308–316. [PubMed: 19377457]
- Robert-Seilaniantz A, Shan L, Zhou JM, Tang X. The *Pseudomonas syringae* pv. *tomato* DC3000 type III effector HopF2 has a putative myristoylation site required for its avirulence and virulence functions. *Mol. Plant Microbe Interact.* 2006; 19:130–138. [PubMed: 16529375]
- Santner A, Calderon-Villalobos LI, Estelle M. Plant hormones are versatile chemical regulators of plant growth. *Nat. Chem. Biol.* 2009; 5:301–307. [PubMed: 19377456]
- Schechter LM, Roberts KA, Jamir Y, Alfano JR, Collmer A. *Pseudomonas syringae* type III secretion system targeting signals and novel effectors studied with a Cya translocation reporter. *J. Bacteriol.* 2004; 186:543–555. [PubMed: 14702323]
- Shan L, Thara VK, Martin GB, Zhou J, Tang X. The *Pseudomonas* AvrPto protein is differentially recognized by tomato and tobacco and is localized to the plant plasma membrane. *Plant Cell.* 2000; 12:2323–2337. [PubMed: 11148281]
- Shedge V, Arrieta-Montiel M, Christensen AC, Mackenzie SA. Plant mitochondrial recombination surveillance requires unusual RecA and MutS homologs. *Plant Cell.* 2007; 19:1251–1264. [PubMed: 17468263]
- Sory M-P, Boland A, Lambermont I, Cornelis GR. Identification of the YopE and YopH domains required for secretion and internalization into the cytosol of macrophages, using the *cyaA* gene fusion approach. *Proc. Natl. Acad. Sci. U.S.A.* 1995; 92:11998–12002. [PubMed: 8618831]
- Tao Y, Xie Z, Chen W, Glazebrook J, Chang HS, Han B, Zhu T, Zou G, Katagiri F. Quantitative Nature of *Arabidopsis* Responses during Compatible and Incompatible Interactions with the Bacterial Pathogen *Pseudomonas syringae*. *Plant Cell.* 2003; 15:317–330. [PubMed: 12566575]
- Tsuda K, Sato M, Glazebrook J, Cohen JD, Katagiri F. Interplay between MAMP-triggered and SA-mediated defense responses. *Plant J.* 2008; 53:763–775. [PubMed: 18005228]
- Van den Ackerveken G, Marois E, Bonas U. Recognition of the bacterial avirulence protein AvrBs3 occurs inside the host plant cell. *Cell.* 1996; 87:1307–1316. [PubMed: 8980236]
- Wei CF, Kvitko BH, Shimizu R, Crabill E, Alfano JR, Lin NC, Martin GB, Huang HC, Collmer A. A *Pseudomonas syringae* pv. *tomato* DC3000 mutant lacking the type III effector HopQ1-1 is able to cause disease in the model plant *Nicotiana benthamiana*. *Plant J.* 2007; 51:32–46. [PubMed: 17559511]
- Xiao Y, Hutcheson SW. A single promoter sequence recognized by a newly identified alternate sigma factor directs expression of pathogenicity and host range determinants in *Pseudomonas syringae*. *J. Bacteriol.* 1994; 176:3089–3091. [PubMed: 8188613]
- Yang B, Zhu W, Johnson LB, White FF. The virulence factor AvrXa7 of *Xanthomonas oryzae* pv. *oryzae* is a type III secretion pathway-dependent nuclear-localized double-stranded DNA-binding protein. *Proc. Natl. Acad. Sci. USA.* 2000; 97:9807–9812. [PubMed: 10931960]
- Yang Y, Gabriel DW. *Xanthomonas* avirulence/pathogenicity gene family encodes functional plant nuclear targeting signals. *Mol. Plant-Microbe Interact.* 1995; 8:627–631. [PubMed: 8589417]
- Yuan J, He SY. The *Pseudomonas syringae* Hrp regulation and secretion system controls the production and secretion of multiple extracellular proteins. *J. Bacteriol.* 1996; 178:6399–6402. [PubMed: 8892851]
- Zhou JM, Chai J. Plant pathogenic bacterial type III effectors subdue host responses. *Curr. Opin. Microbiol.* 2008; 11:179–185. [PubMed: 18372208]
- Zipfel C, Robatzek S, Navarro L, Oakeley EJ, Jones JD, Felix G, Boller T. Bacterial disease resistance in *Arabidopsis* through flagellin perception. *Nature.* 2004; 428:764–767. [PubMed: 15085136]

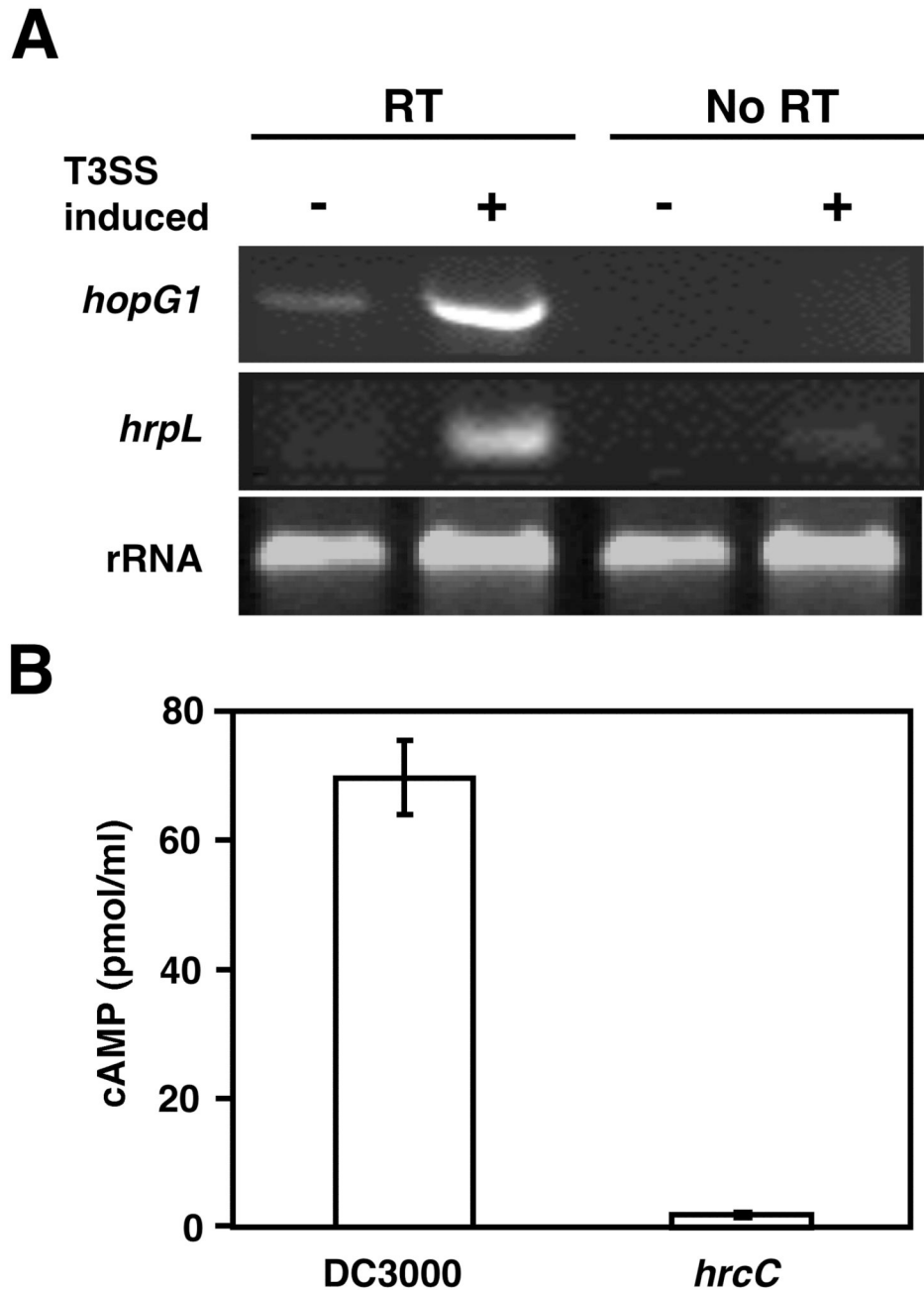


Fig. 1. *hopG1* is expressed in T3SS-inducing conditions and translocated into plant cells via the T3SS

(A) Semi-quantitative RT-PCR of *hopG1* and *hrpL* from DC3000 grown for 3 hours in rich media (-) or in T3SS-inducing minimal media (+). *hopG1* and *hrpL* were expressed at higher levels in T3SS-inducing medium than in rich media indicating that *hopG1* is induced with the T3SS. (B) Adenylate cyclase (CyaA) translocation assay of C-terminal CyaA fusions of HopG1 constitutively expressed in wild type DC3000 and the T3SS deficient DC3000 *hrcC* mutant. The cAMP level indicates the amount of protein injected into plant tissues (the standard errors are indicated, $p < 0.001$). Each experiment was repeated at least twice with similar results.

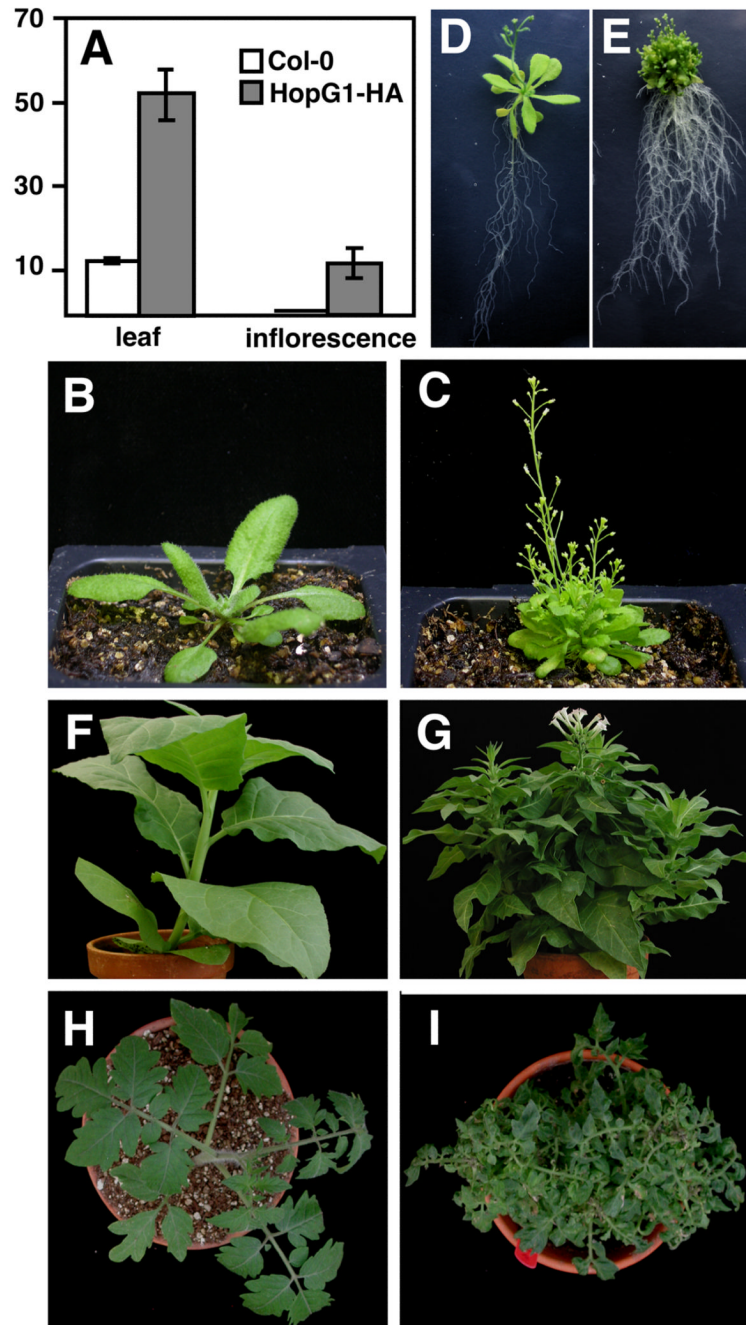


Fig. 2. The constitutive expression of DC3000 HopG1-HA *in planta* causes an altered developmental phenotype

(A) Bar graph showing the number of leaves and inflorescences on wild type *A. thaliana* Col-0 and *A. thaliana* Col-0 expressing HopG1-HA 20 days after germination (the standard errors are indicated, $p < 0.001$). Photographs of *A. thaliana* Col-0 wild type (B) and *A. thaliana* Col-0 expressing HopG1-HA (C) taken 20 days after germination. Five week old *A. thaliana* Col-0 wild type (D) and *A. thaliana* Col-0 expressing HopG1-HA (E) grown on agar MS plates. *N. tabacum* cv. Xanthi (tobacco) wild type (F) and *N. tabacum* cv. Xanthi expressing HopG1-HA (G). *L. esculentum* cv. MoneyMaker (tomato) wild type (H) and *L.*

esculentum cv. Moneymaker expressing HopG1-HA (**I**). Constitutive expression of HopG1-HA in all of these plants led to reduced stature, increased branching, and infertility.

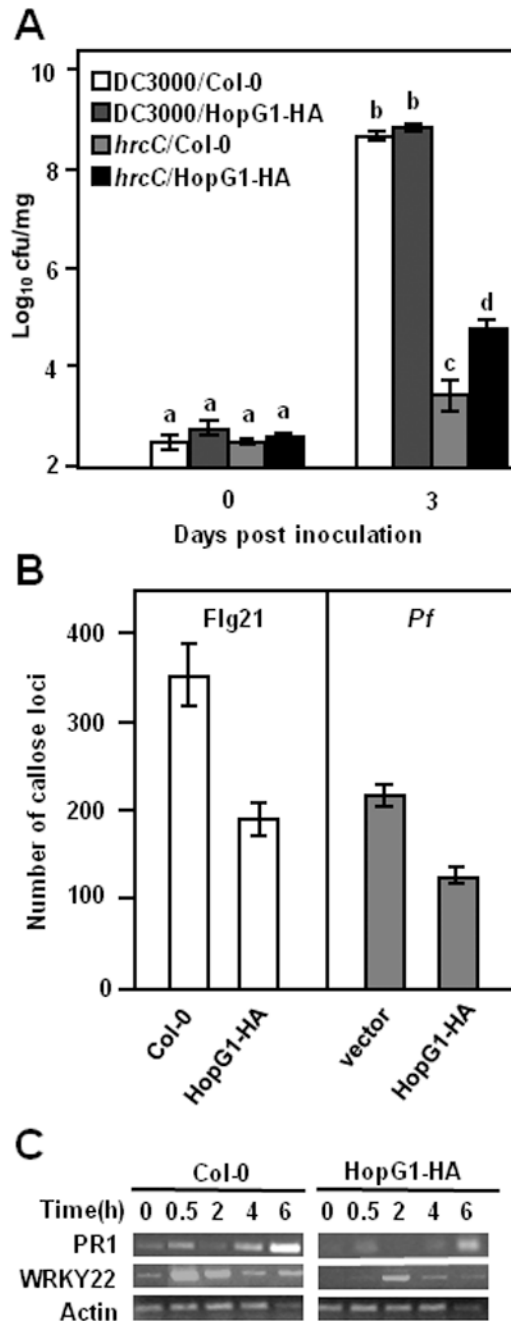


Fig. 3. HopG1-HA suppresses PTI outputs

(A) Wild type and HopG1-HA expressing *A. thaliana* Col-0 were spray-inoculated with 1×10^8 cells/ml of DC3000 or the DC3000 T3SS deficient *hrcC* mutant and bacteria were enumerated at 0 and 3 days after inoculation. No difference in bacterial growth was observed with DC3000 on the HopG1-HA expressing plants, but the *hrcC* mutant showed a greater increase in growth on HopG1-HA expressing plants compared to wild type *A. thaliana* (a, b, c and d are statistically significantly different ($p < 0.01$), standard error is shown). (B) Wild type and HopG1-HA-expressing *A. thaliana* Col-0 plants were infiltrated with the Flg21 peptide from flagellin or wild type *A. thaliana* Col-0 was infiltrated with the PTI-inducing non-pathogen *P. fluorescens* (*Pf*) expressing a *P. syringae* T3SS carrying

hopG1-HA or a vector control. The plant tissue was stained with aniline blue and callose foci were enumerated. These results showed that both *in planta* expressed HopG1-HA and T3SS-injected HopG1-HA can suppress callose deposition ($p < 0.01$). Each experiment was repeated at least twice with similar results and the standard error bars are indicated. (C) Semi-quantitative RT-PCR of pathogen induced genes from wild type and HopG1-HA-expressing *A. thaliana* infiltrated with Flg21. PR1 and WRKY22 were downregulated in HopG1-HA-expressing plants in response to Flg21.

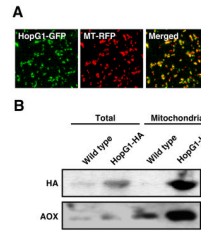


Fig. 4. HopG1 is targeted to plant mitochondria

(A) HopG1 C-terminally fused to the green fluorescence protein (HopG1-GFP) and an N-terminal mitochondrial targeting sequence from isovaleryl-CoA-dehydrogenase fused to the red fluorescent protein eqFP611 (MT-RFP) were transiently co-expressed in tobacco by *Agrobacterium*-mediated transformation and imaged using confocal microscopy. HopG1-GFP, MT-RFP and merged images are shown. The yellow fluorescence in the merged image indicates co-localization of HopG1-GFP and MT-RFP. (B) Subcellular fractionation of mitochondria from wild type and HopG1-HA-expressing tobacco was accomplished using Percoll density gradient centrifugation and the resulting samples were analyzed with immunoblots using antibodies that recognized HA or alternative oxidase (AOX). The immunoblot analysis showed that in plants expressing HopG1-HA it was enriched in the mitochondrial fraction compared to the total protein extract. A non-specific band of a similar size to HopG1-HA is also recognized by the anti-HA antibodies as seen in the wild type total protein extract. Immunoblots against the classic mitochondria marker protein AOX were used to evaluate mitochondrial enrichment. Each experiment was repeated at least twice with similar results.

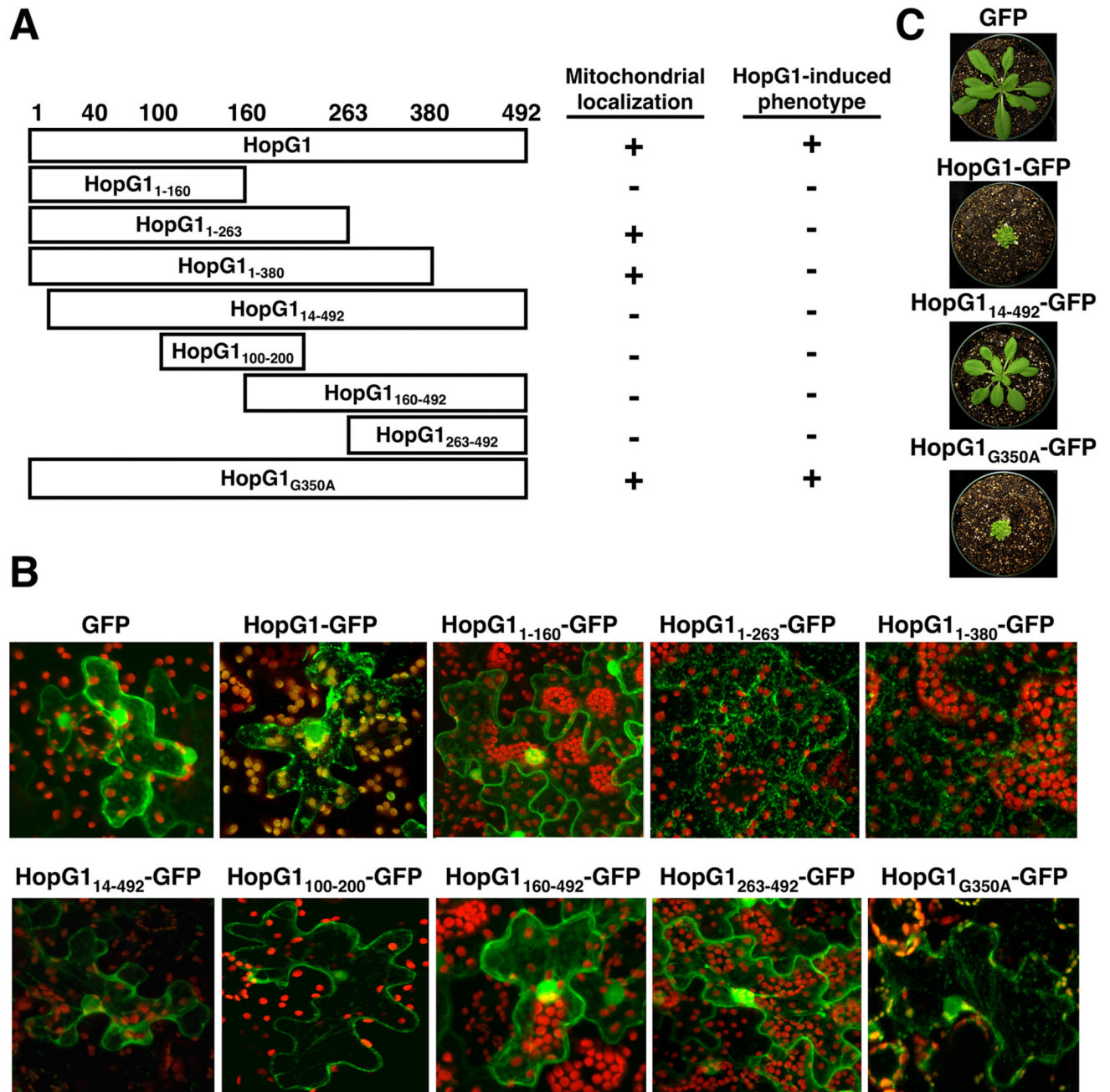


Fig. 5. The mitochondrial targeting sequence of HopG1 is in its N-terminal 263 amino acids (A) A schematic representation of the HopG1-GFP truncations and the HopG1-GFP cyclophilin binding site mutant derivative (HopG1_{G350A}-GFP), their localization to plant mitochondria, and ability to induce the *A. thaliana* developmental phenotype induced by full length HopG1-HA. (B) Confocal micrographs of tobacco cells transiently expressing HopG1-GFP truncations and HopG1_{G350A}-GFP. Only the full length HopG1-GFP, HopG1₁₋₂₆₃-GFP, HopG1₁₋₃₈₀-GFP, and HopG1_{G350A}-GFP were targeted to the mitochondria. Each construct was tested at least twice with similar results. (C) HopG1-GFP truncations and HopG1_{G350A}-GFP were stably transformed into *A. thaliana* Col-0 to test whether they produced the HopG1-induced plant phenotype. Only full length HopG1-GFP

and HopG1_{G350A}-GFP induced the plant developmental phenotype as shown in these representative four week old plants.

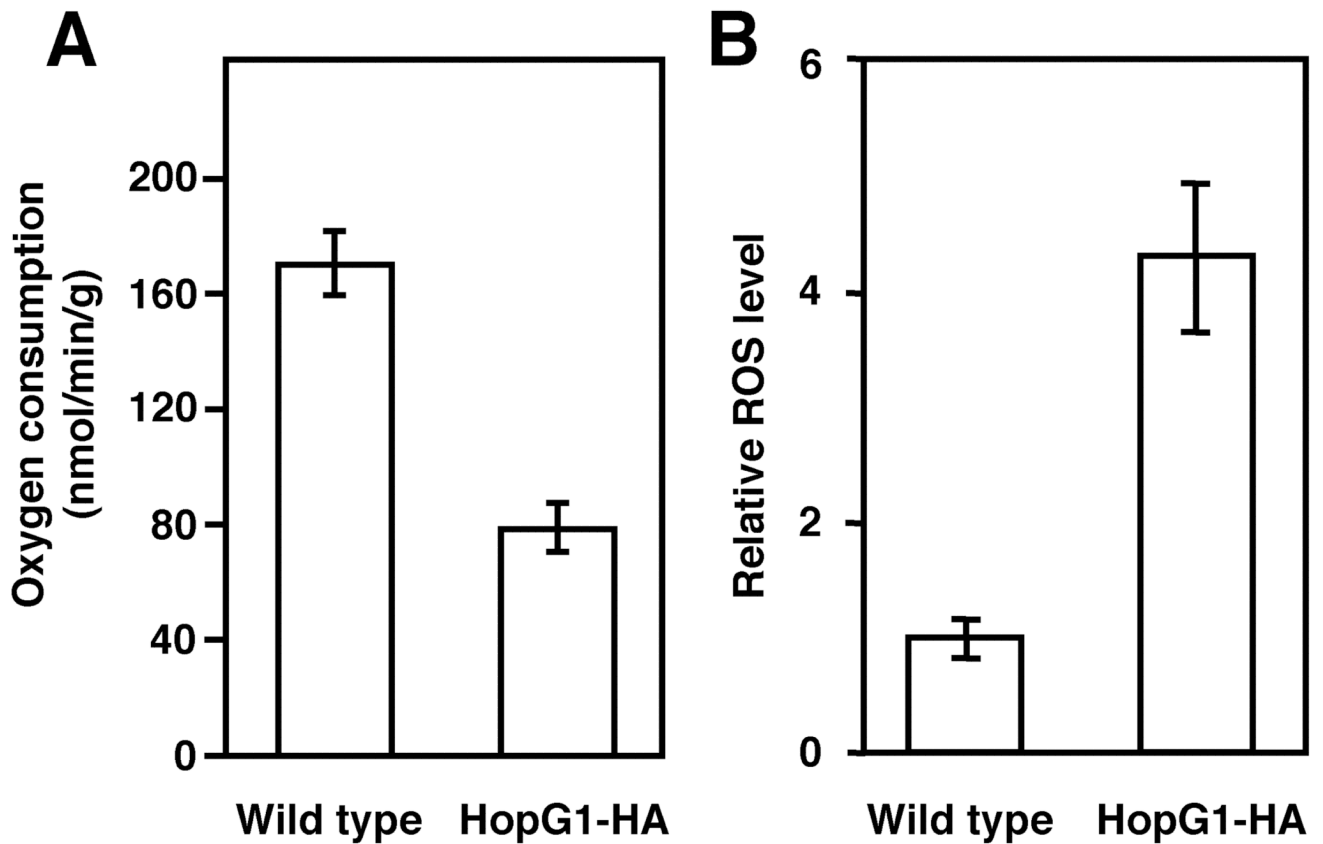


Fig. 6. Plants expressing HopG1-HA exhibit a reduced rate of respiration and increased reactive oxygen species production

(A) Oxygen consumption rates in untreated wild type tobacco and HopG1-HA-expressing tobacco leaf disks were measured in the dark using an oxygen electrode. The rate of oxygen consumption was lower in HopG1-HA-expressing plants ($p < 0.0005$). (B) Relative basal reactive oxygen species (ROS) levels were determined in wild type and HopG1-HA-expressing tobacco leaf extracts by measurement of the relative fluorescence of the ROS-sensitive probe H₂DCFDA and normalizing to total protein content. ROS levels were enhanced in HopG1-HA expressing plants ($p < 0.005$). Each experiment was repeated at least twice with similar results and standard errors are indicated.